International Journal of Physical Research, 6 (1) (2018) 49-52

International Journal of Physical Research

Website: www.sciencepubco.com/index.php/IJPR
doi: 10.14419/ijpr.v6i1.10754
Research paper

Equation of state and some other properties of rock-salt AlN

Salah Daoud [1] *, Rabie Mezouar [2], Abdelfateh Benmakhlouf [3]

[1] Laboratory of Materials and Electronic Systems (LMSE), Mohamed Elbachir El Ibrahimi, Bordj Bou Arreridj University, 34000 Bordj Bou Arreridj, Algeria
[2] Department of Mechanical Engineering, Faculty of Technology, University of Amar Telidji-Laghouat, 03000 Laghouat, Algeria
**Corresponding author E-mail: salah_daoud07@yahoo.fr*

Abstract

The object of the present work is to study the equation of state (EOS) and the temperature dependence of the vibrational constant pressure heat capacity, the adiabatic bulk modulus *Bs* and the pressure derivative of the isothermal bulk modulus of cubic rock-salt Aluminum nitride under high pressure up to 100 GPa. In addition, the isothermal bulk modulus and the Debye temperature θ_D versus pressure at 1800 K are presented. Some structural and thermophysical properties used here are taken from our previous paper published in J. Electron. Mater. (2018) DOI: 10.1007/s11664-018-6169-x. The results obtained are analyzed and compared with other data of the literature.

Keywords: *ALN Semiconductor; Equation of State; Constant-Pressure Heat Capacity; High Pressure.*

1. Introduction

Because of the good performance of Aluminum nitride (AlN) material, it has been widely used in many areas [1]. Having a large electro-mechanical coupling factor and large range temperature stability, as well as a high acoustic wave velocity, AlN material can be used in surface acoustic wave (SAW) devices, such as filters, resonators, actuators and sensors [2].
In normal conditions, AlN semiconductor has the wurtzite (B4) structure, but the synthesis of both cubic zincblende (B3) and rock-salt (B1) meta-stable phases is also possible [3], [4].
Under compression, the B4 phase transforms to B1 structure at around 22.5 GPa [5]. According to the Pressure-Temperature diagram simulation [2], it was found that the minimal pressure stabilizing B1 phase of AlN decreases with increasing of temperature.
Zhang et al. [5] suggest that the AlN with B1 phase is wide band gap semiconductor with an indirect gap of around 4.53 eV.
In our work [6], some elastic and thermophysical properties of AlN with B1 phase under pressure up to 100 GPa were investigate. To extent our study on AlN with cubic rock-salt phase, some other properties have been delivered using the structural parameters and some thermophysical properties of our recent work [6].

2. Theory, results and discussion

2. 1. Normalized structural parameters

For any compressed material, the unit cell volumes at fixed values of applied hydrostatic pressure were usually used to construct the equation of state (EOS). The normalized lattice parameter (a_p/a_0) versus pressure in the range from 0 to 100 GPa for cubic rock-salt AlN was plotted in Fig. 1, along with the theoretical one reported by Zhang et al. [5]. An analytical relation for the pressure dependence of (a_p/a_0) is given by the following a quadratic fit:

$$(a_p/a_0) = 1 - 1.03\times10^{-3}\, p + 3.04\times10^{-6}p^2 \quad (1)$$

From figure 1, we observe that (a_p/a_0) of our material of interest decreases with increasing pressure, where it is started with the value 1 at zero pressure, and it reaches the value 0.927 at 100 GPa.

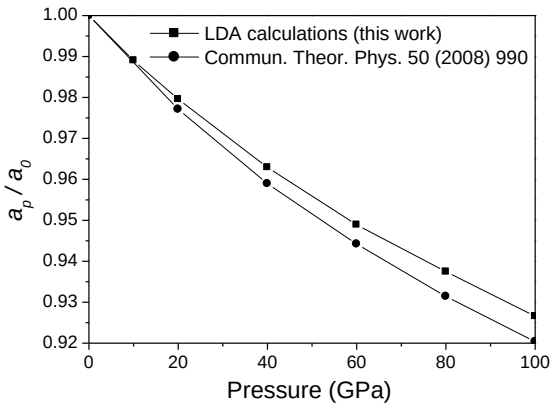

Fig. 1: Normalized Lattice Parameter (a_p/a_0) Versus Pressure.

The calculated normalized volume (V_p/V_0) versus pressure is plotted in Fig. 2, along with the theoretical one reported by Zhang et al. [5]. An analytical relation for the pressure dependence of V_p/V_0 is given by the following a quadratic fit:

$$(V_p/V_0) = 1 - 0.003\, p + 9.94\times10^{-6}p^2 \quad (2)$$

Where p is given in GPa, and (V_p/V_0) is given without unity.
From figure 2, we observe also that V_p/V_0 decreases with increasing pressure, where it also started with the value 1 at zero pressure, and it reaches the value 0.796 at 100 GPa. From the curves of Figs. 1 and 2, it can be seen that the compressibility of the material calculated in this work is smaller than that reported by Zhang et al. [5]. This, because Zhang et al. [5] used the generalized gradient approximation (GGA) to describe the quantum mechanical exchange-correlation effects, whereas the local density approximation (LDA) was used here. We can note that the LDA

gives a larger bulk modulus (lower compressibility) and smaller lattice parameter than the GGA.

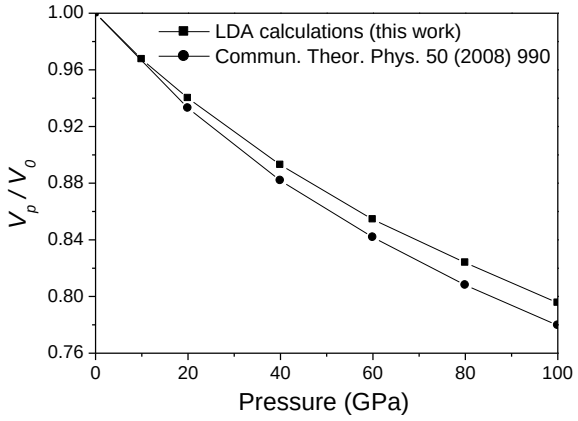

Fig. 2: Normalized Volume (V_p/V_0) Versus Pressure.

The EOS parameters (equilibrium lattice constant a_0, bulk modulus B_0, and its pressure derivatives B_0') can be determined through the well-known pressure normalized-volume (P-(V/V_0)) third-order Vinet EOS, which is given as follow [7]:

$$P(V) = 3B_0 \left[\frac{1-(V/V_0)^{1/3}}{(V/V_0)^{2/3}}\right] exp\left\{\frac{3}{2}(B_0' - 1)\left[1-\left(V/V_0\right)^{1/3}\right]\right\} \quad (3)$$

Where: V is the volume at pressure P, and V_0 is the volume at zero-pressure, respectively.
The calculated data (P-(V/V_0)) of AlN material with B1 structure in the range from 0 to 100 GPa was plotted in Fig. 3.

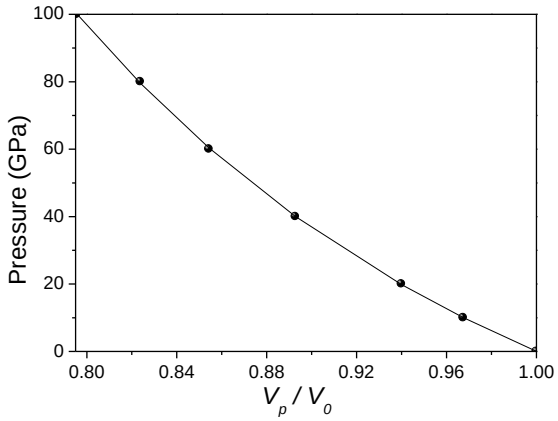

Fig. 3: Pressure Versus (V_p/V_0) of AlN with B1 Structure.

The obtained values of a_0, B_0, and B_0' are given in Table 1, and compared with the experimental [4] and other theoretical data [5], [6], and [8] of the literature.

Table 1: Equilibrium Lattice Constant a_0, Bulk Modulus B_0, and Its Pressure Derivatives B_0' of AlN, Compared to the Experimental [4] and Other Theoretical Data [5], [6], [8]

Parameter	a_0 (Å)	B_0 (GPa)	B_0'
This work	4.025	284.02	3.89
Ref. [4]	4.064	295 ± 17	3.5 ± 0.4
Ref. [5]	4.068	-	-
Ref. [6]	4.026	275.14	3.68
Ref. [8]	4.016	268.47	4.12

In general, our calculated values of a_0, B_0 and B_0' of cubic rock-salt AlN semiconductor are agree best with the experimental ones [4] and other theoretical data [5], [6] and [8]; where for example the deviation of B_0 between our calculation (284.02 GPa) and the experimental one (295 GPa) [4] is only about 3.73 %. It can be seen that our value (3.89) of B_0' is slightly higher than our previous result (3.68) [6] obtained from the energy - volume data, but it localized in the range of other data reported in the literature.

2.2. Crystal density

The calculated crystal density at different values of pressure is plotted in Fig. 4, along with the theoretical one calculated from the work of Zhang et al. [5]. An analytical relation for the pressure dependence of the density is given by the following a quadratic fit:

$$g = 4.181 + 1.348\times10^{-2}\, p - 0.285\times10^{-4} p^2 \quad (4)$$

Where p is given in GPa, and g in g/cm^3.

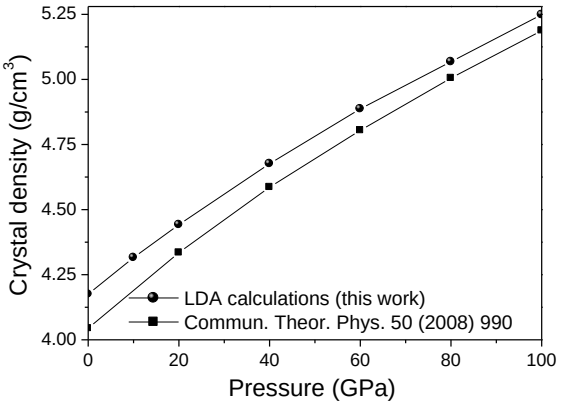

Fig. 4: Crystal Density versus Pressure Up to 100 GPa.

From figure 1, we observe clearly that the density g increases with increasing pressure, where it beginning with the value 4.175 g/cm^3 at zero pressure, and it reaches the value 5.249 g/cm^3 at 100 GPa.

2.3. Vibrational constant pressure heat capacity

Several thermodynamic quantities are related to the elastic constants of solid [6]. The constant pressure heat capacity Cp was usually expressed as a function of the enthalpy H as follow [9]: $Cp = (dH/dT)_P$, where, T is the absolute temperature, and P is the pressure. In the quasi-harmonic Debye model approximation, the vibrational constant pressure heat capacity Cp and the constant volume heat capacity Cv are related by the following formula [10]

$$Cp = Cv\,(1+\alpha\,\gamma\,T) \quad (5)$$

Where, α is the volumetric thermal expansion coefficient, γ is the Grüneisen parameter, and T is the temperature.
Figure 5 shows the dependence of the vibrational constant pressure heat capacity Cp as a function of temperature at three different pressures (0 GPa, 50 GPa, and 100 GPa).

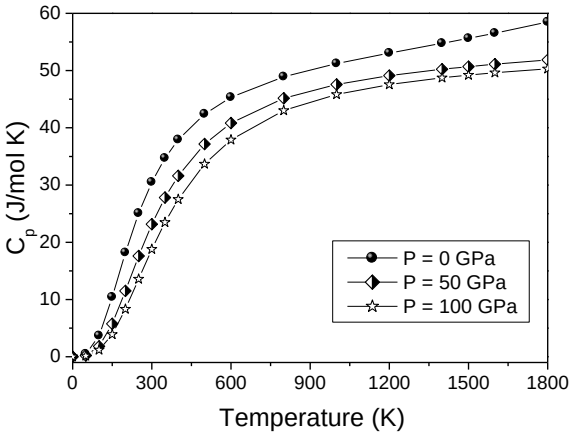

Fig. 5: Variations of Cp with Temperature of AlN with B1 Structure at Various Pressures (0 GPa, 50 GPa, and 100 GPa).

From figure 5, we can observe that Cp increases with increasing of the temperature and decreases with arising of pressure. It is also clear that the increasing tendency of Cp as a function of temperature is somewhat similar at 0 GPa, 50 GPa, and 100 GPa.
Figure 6 shows the dependence of the constant pressure heat capacity Cp as a function of pressure at three different temperatures (300 K, 600 K, and 1800 K).

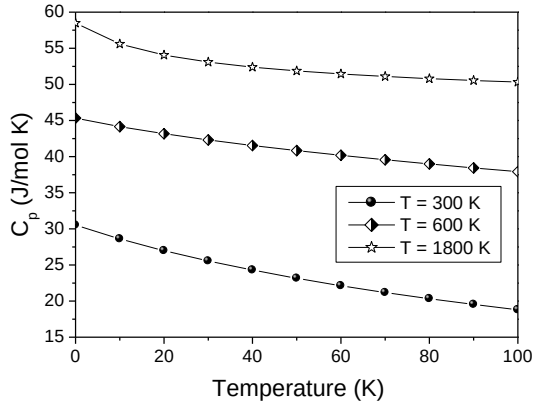

Fig. 6: Variations of Cp with Pressure at Various Temperatures.

From Fig. 6, we can observe that Cp decreases almost linearly (especially at high pressure) with increasing of pressure. At P = 0 and T = 300 K, our value of Cp is around 30.52 J/mol K, whereas at 1800 K, it reaches the value 58.48 J/mol K. The decreasing tendency of Cp as a function of pressure is very slowly at 1800 K.
2.4. Pressure derivative of isothermal bulk modulus
The first order pressure derivative of the isothermal bulk modulus B_T' at given pressure and temperature is a very important parameter for the high-pressure studies [11]. Figure 7 shows the dependence of B_T' of AlN with B1 structure as a function of pressure at different temperatures. We can observe that B_T' decreases with increasing of pressure, and increases with increasing of the temperature. At zero pressure and zero temperature, our predicted value of the pressure derivative of B_T is around 4.05, whereas at 1500 K, it reaches the value 5.37.

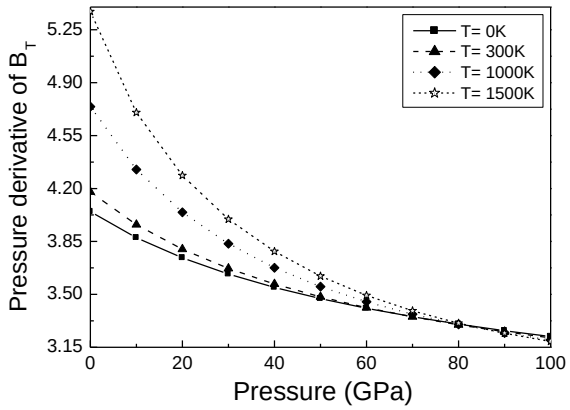

Fig. 7: Pressure Derivative of Isothermal Bulk Modulus versus Pressure of Aln with B1 Structure at Various Temperatures.

From figure 7, we can observe also that the effect of the temperature on the pressure derivative of B_T becomes almost negligible, where for the values of pressure more than 80 GPa, all the curves of this later become superposed for all temperatures.

2.5. Isothermal bulk modulus and Debye temperature

Fig. 8 shows the dependence of the isothermal bulk modulus B_T and the Debye temperature θ_D as a function of pressure at 1800 K. We can observe that both B_T and θ_D increase with increasing pressure. The same behavior was observed for TlP material at zero-temperature [12]. At zero pressure, our predicted value of B_T is around 187.61 GPa, whereas that of θ_D is around 901.1 K.

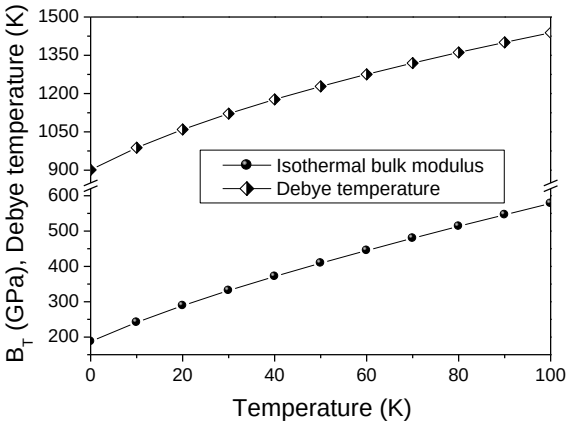

Fig. 8: Isothermal Bulk Modulus B_T and Debye Temperature Θ_D versus Pressure of AlN with B1 Structure at 1800 K.

Two analytical relations for the pressure dependence of B_T and θ_D are given by the following a quadratic fits:

$$B_T = 192.11 + 4.88\ p - 1.04\times10^{-2}p^2 \quad (6)$$

$$\theta_D = 910.65 + 7.54\ p - 2.33\times10^{-2}p^2 \quad (7)$$

Where p and B_T are given in GPa, and θ_D is given K.

2.6. Adiabatic bulk modulus

Similarly to the vibrational constant pressure heat capacity Cp and the vibrational constant volume heat capacity Cv, in the quasi-harmonic Debye model approximation, the adiabatic bulk modulus Bs and isothermal bulk modulus B_T are related by the following formula [10]

$$Bs = B_T(1+\alpha\,\gamma\,T) \quad (8)$$

Where, α is the volumetric thermal expansion coefficient, γ is the Grüneisen parameter, and T is the temperature.
Figure 9 shows the dependence of the adiabatic bulk modulus Bs as a function of temperature at different pressures (0 GPa, 50 GPa, and 100 GPa). From figure 9, we can observe that Bs decreases very slowly with increasing of the temperature and at pressure of 100 GPa, it is almost unchangeable with arising of the temperature. It is also clear that the increasing tendency of Bs as a function of temperature is somewhat similar at 50 GPa and 100 GPa.

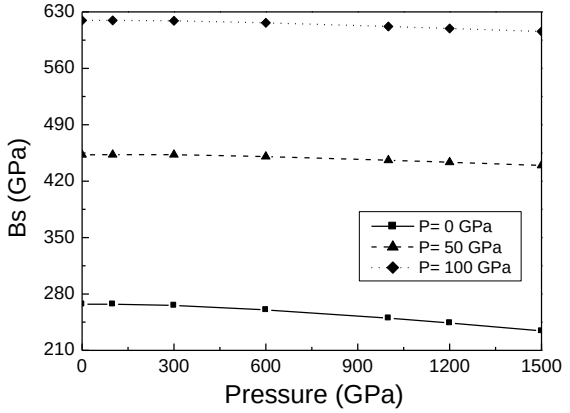

Fig. 9: Variations of Bs with Temperature of AlN with B1 Structure at Various Pressures (0 GPa, 50 GPa, and 100 GPa).

Figure 10 shows the dependence of the adiabatic bulk modulus Bs as a function of pressure at four different temperatures (0 K, 300

K, 1000 K, and 1500 K). From figure 10, we can observe that Bs increases almost linearly with increasing of pressure.

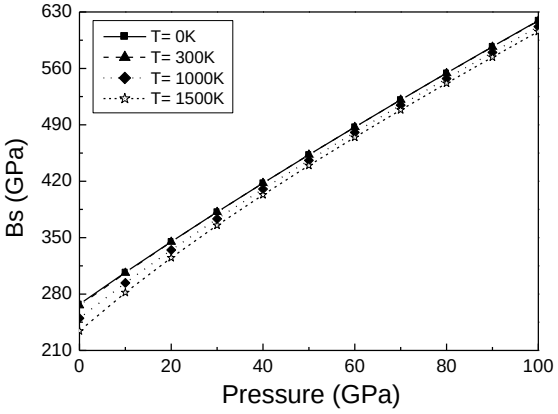

Fig. 10: Variations of Bs with Pressure of AlN with B1 Structure at Various Temperatures (0 K, 300 K, 1000 K, and 1500 K).

At zero pressure and T = 300 K, our predicted value of Bs is around 265.88 GPa, whereas at 1500 K, it reaches the value 234.13 GPa. Compared to bulk modulus B_T, this later is around 262.7 GPa at zero pressure and T = 300 K, and it reaches the value about 206 GPa at T = 1500 K [6]. So the introduction of the temperature effect (T = 1500 K) increases the bulk modulus from the value 206 GPa (B_T) to the value 234.13 GPa (Bs).

Figure 11 shows the dependence of the adiabatic bulk modulus Bs and the isothermal bulk modulus B_T [6] as a function of pressure at 1500 K. From figure 11, we can observe that Bs increases almost linearly with increasing of pressure.

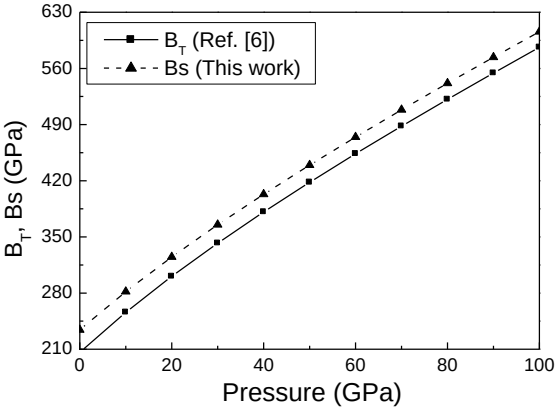

Fig. 11: Variations of B_T [6] and Bs with Pressure of AlN with B1 Structure at 1500 K.

From figure 11, we can observe that the temperature of 1500 K, affect considerably the behavior of our material of interest, where for example zero pressure, our predicted value of Bs is around 234.13GPa, whereas that of B_T, is around 206 GPa [6].

3. Conclusion

Using some structural and thermophysical properties published previously in J. Electron. Mater. (2018) DOI: 10.1007/s11664-018-6169-x, we determine the EOS parameters (equilibrium lattice constant, bulk modulus, and its pressure derivatives) and the crystal density of cubic rock-salt AlN using the pressure-volume data. The values obtained are in general in good agreement with the experimental ones and other theoretical results of the literature.

In addition the pressure and temperature dependence of the vibrational constant pressure heat capacity Cp, the adiabatic bulk modulus Bs and the pressure derivative of the isothermal bulk modulus B_T' under high temperature and high pressure up to 100 GPa are also studied. It was found that the effect of the temperature on B_T' becomes almost negligible for very high pressure (more than 80 GPa).

The adiabatic bulk modulus Bs increase almost linearly with increasing pressure and decreases very slowly with the temperature.

The isothermal bulk modulus B_T and the Debye temperature θ_D versus pressure at 1800 K are also presented. It was found that both B_T and θ_D increase with increasing pressure.

Hope, in the future, other efforts will be focused on the preparation and investigation of AlN with B1 structure to characterize it for its mechanical, optical, and electrical properties and to be useful for device fabrication.

References

[1] X. Tan, Z. Xin, X. Liu, and Q. Mu, "First-principles study on elastic properties of AlN", Advanced Materials Research, Vols. 821-822, (2013), pp. 841-844. https://doi.org/10.4028/www.scientific.netAM R.821-822.841.

[2] V.S. Kudyakova, R.A. Shishkin, A.A. Elagin, M.V. Baranov, A.R. Beketov, "Aluminium nitride cubic modifications synthesis methods and its features. Review", Journal of the European Ceramic Society, Vol. 37, No. 4, (2016), pp. 1143-1156. https://doi.org/10.1016/j.jeurceramsoc.2016.11.051.

[3] X.P. Hao, M.Y. Yu, D.L. Cui, X.G. Xu, Y.J. Bai, Q.L. Wang, and M.H. Jiang, "Synthesize AlN nanocrystals in organic solvent at atmospheric pressure", Journal of Crystal Growth, Vol. 242, No. 1-2, (2002) pp. 229-232. https://doi.org/10.1016/S0022-0248(02)01369-6.

[4] L. H. Shen, X. F. Li, Y. M. Ma, K. F. Yang, W. W. Lei, Q. L. Cui, and G. T. Zou, " Pressure-induced structural transition in AlN nanowires", Applied Physics Letters. Vol. 89, No. 14, (2006) pp. 141903 (3 pages). https://doi.org/10.1063/1.2358125.

[5] W. Zhang, X-R. Chen, L-C. Cai, and Q-Q. Gou, "Electronic and optical properties of rock-salt AlN under high pressure via first-principles analysis", Communications in Theoretical Physics. Vol.50, (2008). pp. 990-994. https://doi.org/10.1088/0253-6102/50/4/41.

[6] N. Lebga, S. Daoud, X-W. Sun, N. Bioud, and A. Latreche, "Mechanical and thermophysical properties of cubic rock-salt AlN under high pressure", Journal of Electronic Materials, Vol. xx, No. xx, (2018), pp. xxx-xxx. https://doi.org/10.1007/s11664-018-6169-x.

[7] A. R. Oganov, J.P. Brodholt, and G.D. Price, Ab initio theory of thermoelasticity and phase transitions in minerals. EMU Notes in Mineralogy Vol. 4, Chapter 5 ('Energy Modeling in Minerals', edited by C.M. Gramaccioli), (2002). pp.83-170

[8] S. Louhibi-Fasla, H. Achour, K. Kefif, and Y. Ghalem, "First-principles Study of high-pressure phases of AlN", Physics Procedia Vol. 55, (2014) pp. 324-328. https://doi.org/10.1016/j.phpro.2014.07.047.

[9] T. Tsuji, Heat capacity of solids, Chapter 5, in Thermodynamic properties of solids, edited by S. L. Chaplot, R. Mittal, and N. Choudhury, WILEY-VCH Verlag GmbH & Co. KGaA, Weinheim, (2010). pp. 159-196, ISBN: 978-3-527-40812-2.

[10] M.A. Blanco, E. Francisco, and V. Luaña, " GIBBS: Isothermal-isobaric thermodynamics of solids from energy curves using a quasi-harmonic Debye model", Computer Physics Communications, Vol.158, (2004), pp. 57-72. https://doi.org/10.1016/j.comphy.2003.12.001.

[11] Z-J. Liu, X-W. Sun, C-R. Zhang, J-B Hu, T. Song, and J-H. Qi, "Elastic tensor and thermodynamic property of magnesium silicate perovskite from first-principles calculations", Chinese Journal of Chemical Physics, Vol.24, No. 6, (2011), pp. 703-711. https://doi.org/10.1088/1674-0068/24/06/703-710

[12] .S. Daoud, "Mechanical and piezoelectric properties, sound velocity and Debye temperature of thallium-phosphide under pressure", International Journal of Advanced Research in Physical Science, Vol. 1, No. 6, (2014), pp. 1-11. www.arcjournals.org/pdfs/ijarps/v1i6/1.pdf.